

# Collisional excitation of monodeuterated ammonia NH<sub>2</sub>D by helium

L. Machin and E. Roueff

Laboratoire Univers et Théories and UMR 8102, Observatoire de Paris-Meudon, 5 place Jules Janssen, 92195 Meudon, France  
e-mail: [leandre.machin;evelyne.roueff]@obspm.fr

Received 13 July 2006 / Accepted 21 August 2006

## ABSTRACT

**Context.** Observations of deuterated molecules are useful probes of the physical and chemical conditions in star-forming regions. However their detailed interpretation is hampered by the lack of knowledge of the corresponding collisional rate coefficients.

**Aims.** We extend our previous study of ammonia collisional excitation by helium to monodeuterated ammonia NH<sub>2</sub>D, which has been found to be abundant in a variety of environments.

**Methods.** We introduce the principal isotopic effects in the collisional equations by calculating the relevant angular dependence of the intermolecular potential energy surface.

**Results.** Cross sections are calculated in the coupled states approximation, and collisional rate coefficients are given from 5 to 100 K, a range of temperatures that is relevant in the interstellar medium.

**Conclusions.** These results allow to include justifiable collisional excitation rate coefficients of NH<sub>2</sub>D by He in the analysis of the emitted radiation for the first time

**Key words.** ISM: general – ISM: molecules – molecular data – molecular processes – scattering

## 1. Introduction

Ammonia NH<sub>3</sub> is the first polyatomic molecule observed in the interstellar medium via centimetric transitions arising within its 1<sub>1</sub> inversion doublet (Cheung et al. 1968). Pure rotational transitions of ammonia that arise in the submillimeter region are not observable from the ground, and the fundamental rotational 1<sub>0</sub> → 0<sub>0</sub> transition of NH<sub>3</sub> at 572.5 GHz was first detected by Liseau et al. (2003) and Larsson et al. (2003) with the space submillimeter telescope ODIN toward the low-mass interstellar cloud core ρ Oph A and the Orion bar. Deuterated isotopomers of ammonia are interesting because, due to their higher reduced mass, the rotational levels become closer in energy and cover a lower frequency domain. Consequently, the rotational transitions of these deuterated forms are in a range of frequencies that is not absorbed by the Earth's atmosphere. Mono-deuterated ammonia NH<sub>2</sub>D was first observed by Turner et al. (1978) in the molecular cloud Sgr B2 by means of its 1<sub>11</sub>–1<sub>01</sub> *ortho* transition at 85.9 GHz. This transition and its associated *para* transition at 110.1 GHz were more recently observed by Tiné et al. (2000) in the dark clouds TMC1 and L134N. Simultaneously, Saito et al. (2000) reported the observations of the *para* transition at 110.1 GHz in several cloud cores. Finally Shah & Wootten (2001) reported a survey of these two lines toward protostellar cores in low-mass star formation regions of the Galaxy.

These observations created a need for collision rate coefficients in order to correctly interpret the different lines and compute kinetic temperature and densities of the molecular component of the ISM via an appropriate treatment of the radiative transfer. Moreover, the future infrared and submillimeter spatial telescope HERSCHEL and the construction of ALMA (Atacama

Large Millimeter Array) in Chile increase the need for these detailed molecular data.

The new accurate intermolecular potential energy surface (PES) for NH<sub>3</sub>-He of Hodges & Wheatley (2001) has been used to reevaluate the collisional excitation of NH<sub>3</sub> by He (Machin & Roueff 2005). As long as the Born-Oppenheimer approximation can be applied, the same PES can be used for any isotopic substitution of the nuclei because the electrostatic interaction depends only on the relative positions of the electrons and the nuclear charges. However, the center of mass reference frame is modified and the expansion coefficients of the PES over the spherical harmonics,  $v_{\lambda\mu}$ , are changed accordingly, as shown in Sect. 2. As NH<sub>2</sub>D is no longer a symmetric top like NH<sub>3</sub>, the formalism of the collision with He is also different and is presented in Sect. 3. The cross sections and the corresponding reaction rate coefficients of the NH<sub>2</sub>D-He system are given respectively in Sects. 4 and 5. We present our conclusion in Sect. 6.

## 2. Potential energy surface

We use the MOLSCAT code version 14 of J. M. Hutson and S. Green to compute the quantal excitation cross sections of NH<sub>2</sub>D by He. The electronic potential that describes the interaction between NH<sub>2</sub>D and He depends only on the relative positions of electronic and nuclear charges involved in the system. The nuclear charges are the same for any isotopic substitution. Then, the PES describing the NH<sub>3</sub>-He system can be used when non adiabatic coupling between electronic and nuclear motion can be neglected (Born-Oppenheimer approximation). We use the recent accurate PES for NH<sub>3</sub>-He of Hodges & Wheatley (2001) as in our previous work on NH<sub>3</sub>-He (Machin & Roueff 2005).

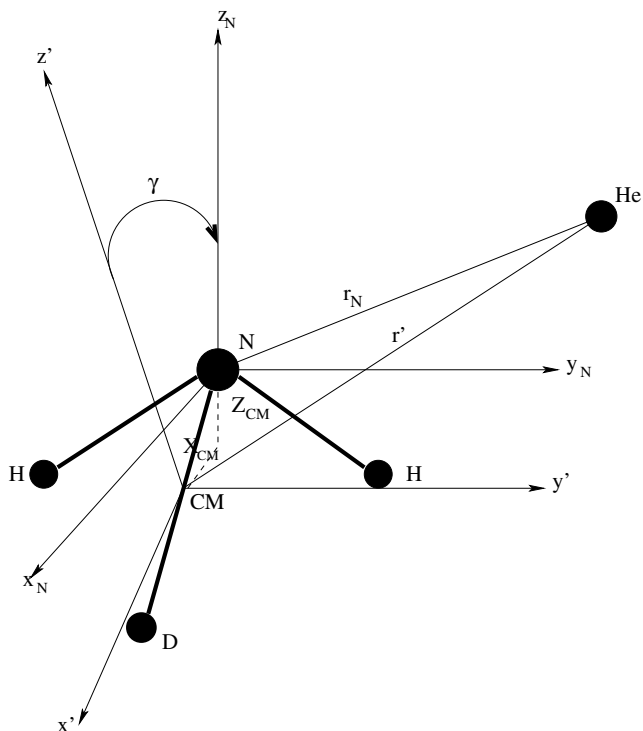


**Fig. 1.** Relation between the center of mass reference frame ( $x', y', z'$ ) of NH<sub>2</sub>D and the reference frame used by Hodges & Wheatley (2001) for their NH<sub>3</sub>-He PES ( $x_N, y_N, z_N$ ).  $X_{CM}$  and  $Z_{CM}$  are the coordinates of the center of mass of NH<sub>2</sub>D in the PES reference frame.  $\gamma$  is the angle between the  $z_N$  and the  $z'$  axis. CM indicates the center of mass and N the nitrogen atom.

This PES is given in a Cartesian coordinate system ( $x_N, y_N, z_N$ ) centered on the nitrogen atom, and the  $z$  axis is collinear to the axis of symmetry ( $C_3$ ) of the NH<sub>3</sub> molecule. This axis is perpendicular to the plane of the three hydrogen atoms. However, the collisional equations to be solved in the MOLSCAT program are written in the center of mass system of the molecule (NH<sub>2</sub>D) with axes equal to those of the principal inertia momenta noted ( $x', y', z'$ ). Figure 1 illustrates the relation between the two reference frames.

We express the PES of Hodges & Wheatley (2001) in the MOLSCAT coordinate system. For NH<sub>2</sub>D, the transformation is the following:

$$x_N = x' \cos(\gamma) - z' \sin(\gamma) + X_{CM} \quad (1)$$

$$y_N = y' \quad (2)$$

$$z_N = x' \sin(\gamma) + z' \sin(\gamma) + Z_{CM}, \quad (3)$$

where  $\gamma$  is the angle between the  $z_N$  and the  $z'$  axes and  $X_{CM}$  and  $Z_{CM}$  are the coordinates of the center of mass of NH<sub>2</sub>D in the PES reference frame ( $x_N, y_N, z_N$ ). The values of  $\gamma$ ,  $X_{CM}$ , and  $Z_{CM}$  are given in Table 1.  $\gamma$  is taken from Cohen & Pickett (1982).  $X_{CM}$  and  $Z_{CM}$  are calculated for an umbrella angle  $\alpha_e = 112.14^\circ$  and for the length of the N-H bond  $r_e = 1.9132 a_0$ . These values correspond to the experimental equilibrium geometry given by Benedict et al. (1957) and reported in Hodges & Wheatley (2001). We expand the PES in the body-fixed coordinates as:

$$V(r', \theta', \phi') = \sum_{\lambda\mu} v_{\lambda\mu}(r') Y_{\lambda\mu}(\theta', \phi'). \quad (4)$$

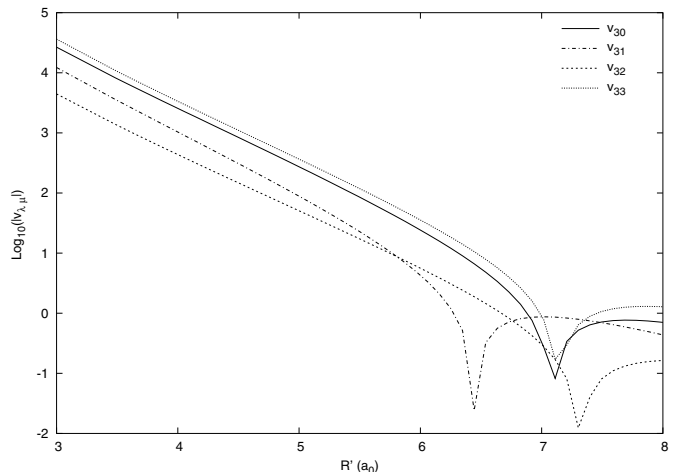


**Fig. 2.**  $v_{\lambda\mu}$  radial coefficients for  $\lambda = 3$  of the PES expansion for NH<sub>2</sub>D. The decimal logarithms of the absolute value of the coefficients, expressed in reciprocal centimeters, are displayed.

**Table 1.** Values of  $\gamma$ ,  $X_{CM}$ , and  $Z_{CM}$  for NH<sub>2</sub>D in the PES reference frame.

Parameter	NH <sub>2</sub> D
$\gamma$ (in degrees)	-8.57
$X_{CM}$ ( $a_0$ )	0.0988
$Z_{CM}$ ( $a_0$ )	-0.1611

In the case of NH<sub>3</sub>, only  $v_{\lambda\mu}(r')$  with  $\mu = 3n$  are non-zero due to the  $C_{3v}$  symmetry. For NH<sub>2</sub>D, this symmetry is broken, so all the  $v_{\lambda\mu}(r')$  have to be included. We use the “VRTP” procedure in the MOLSCAT program, which provides the expansion coefficients  $v_{\lambda\mu}(r')$  of the PES. Decimal logarithms of the absolute values corresponding to  $\lambda = 3$  coefficients are displayed in Fig. 2. The cusps in the figure correspond to a change of sign as the coefficients become negative at large distances. We see that for  $v_{3\mu}$  with  $\mu = 1$  and  $\mu = 2$  coefficients are not negligible compared with the  $v_{3\mu}(r')$  with  $\mu = 0$  and  $\mu = 3$ . In the present calculations, we have included  $v_{\lambda\mu}(r')$  until  $\lambda = 10$ , which allows a satisfactory representation of the PES.

### 3. Collisional treatment

NH<sub>2</sub>D is an asymmetric top and is treated as a rigid rotator. The relevant formalism of collisional excitation of asymmetric tops is described in Garrison et al. (1976), Garrison & Lester (1977), and Palma & Green (1987). Two different reference frames are introduced: the body-fixed (BF) frame ( $x', y', z'$ ), which corresponds to the principal moments of inertia axes system, and the space-fixed (SF) frame ( $x, y, z$ ), which both have their origin at the center of mass of the molecule. The BF axes are connected to the SF axes by a rotation involving the Euler angles ( $\alpha\beta\gamma$ ). The rotational Hamiltonian introduced in MOLSCAT is taken as:

$$H_{\text{asymtop}} = AJ_x'^2 + BJ_y'^2 + CJ_z'^2 - D_{jj}J^4 - D_{jk}J^2J_z'^2 - D_{kk}J_z'^4. \quad (5)$$

$J_{x',y',z'}$  represents the components of the rotational angular momentum in the BF reference frame oriented along the principal moments of inertia of the molecule ( $I_{x',y',z'}$ ). The rotational constants are given by  $A = \hbar^2/2I_{x'}$ ,  $B = \hbar^2/2I_{y'}$ , and  $C = \hbar^2/2I_{z'}$ , and only the first three distortion terms are included. The numerical values are displayed in Table 2. The rotational constants are from CDMS (Müller et al. 2001) and the distortion terms from

**Table 2.** Values of the rotational constants  $A$ ,  $B$ , and  $C$ , and of the centrifugal distortion constants  $D_{jj}$ ,  $D_{jk}$ , and  $D_{kk}$  for NH<sub>2</sub>D used in this work in units of cm<sup>-1</sup>.

$A$	9.6759
$B$	6.4103
$C$	4.6968
$D_{jj}$	$5.2772 \times 10^{-4}$
$D_{jk}$	$-7.9872 \times 10^{-4}$
$D_{kk}$	$3.6537 \times 10^{-4}$

**Table 3.** Energy term values of the rotational levels of NH<sub>2</sub>D calculated by MOLSCAT with the rotational and distortion constants of Table 2.

Rotational level	Energy (cm <sup>-1</sup> )
0 <sub>00</sub>	0.0000
1 <sub>01</sub>	11.1062
1 <sub>11</sub>	14.3718
1 <sub>10</sub>	16.0841
2 <sub>02</sub>	32.7961
2 <sub>12</sub>	34.8677
2 <sub>11</sub>	39.9993
2 <sub>21</sub>	49.7961
2 <sub>20</sub>	50.3112
3 <sub>03</sub>	64.2795

Coudert et al. (1986). The derived energy term values of the ten first rotational levels are displayed in Table 3.

To solve the nuclear rotational Schrödinger's equation, it is convenient to expand the asymmetric top wave functions on the symmetric top wave functions.

$$|j\tau m\rangle = \sum_{k=-j}^j a_{k\tau}^j |jkm\rangle, \quad (6)$$

where  $|jkm\rangle$  are defined as in Green (1976):

$$|jkm\rangle = \sqrt{\frac{2j+1}{8\pi^2}} \mathcal{D}_{km}^j(\alpha\beta\gamma), \quad (7)$$

where  $j$ ,  $k$ , and  $m$  are, respectively, the eigenvalues of  $J^2$ ,  $J_z'$ , and  $J_z$ . The  $a_{k\tau}^j$  are the expansion coefficients that are calculated in the MOLSCAT program for the value ITYPE = 6.  $\tau$  is an index that labels the asymmetric top rotational states. The ortho and para character of NH<sub>2</sub>D levels arises when one takes the overall symmetry of the wavefunction under the exchange of the two protons into account. The result is a removal of the degeneracy without including the inversion operation. However, the corresponding level energies are very close (see, for example, the values summarized in Coudert & Roueff 2006). We do not include the corresponding terms in the Hamiltonian. So, the ortho and para levels are degenerate in our treatment and the corresponding excitation probabilities within the ortho and para symmetry will be identical. In addition, the ortho-para excitation is strictly forbidden. The total Hamiltonian of the system is expressed as:

$$H = -\frac{\hbar^2}{2\mu} \nabla_r^2 + H_{\text{asymtop}}(\hat{R}') + V(r, \hat{R}'), \quad (8)$$

where the first term is the kinetic energy operator, the second is the asymmetric top Hamiltonian, and the third the PES.  $\mu$  is the reduced mass of the system NH<sub>2</sub>D-He. The value of  $\mu$  is taken as 3.2754 amu.  $\mathbf{r} = (r, \theta, \phi)$  is the position of the helium atom

in the SF frame, and  $\hat{R}' = (\alpha\beta\gamma)$  is the orientation of the NH<sub>2</sub>D molecule in the SF frame. The position of He in the BF frame is given by  $\mathbf{r}' = (r', \theta', \phi')$  with  $r' = r$ . Then we have to solve the Schrödinger's equation:

$$H\Psi = E_{\text{tot}}\Psi, \quad (9)$$

where  $E_{\text{tot}}$  is the total collision energy and  $\Psi$  the total eigenfunction that includes the coupling of the rotational angular momentum  $\mathbf{j}$  and the relative orbital angular momentum  $\boldsymbol{\ell}$  of the helium atom to obtain the total angular momentum  $\mathbf{J} = \mathbf{j} + \boldsymbol{\ell}$ .  $\Psi$  is defined by:

$$\Psi_{j\ell\tau}^{JM}(\mathbf{r}, \hat{R}') = \sum_{j'\ell'\tau'} \frac{1}{r} u_{j'\ell'\tau'}^{Jj\ell\tau}(r) |JMj'\ell'\tau'\rangle, \quad (10)$$

$u_{j'\ell'\tau'}^{Jj\ell\tau}(r)$  is the radial part of the wavefunctions, and  $|JMj'\ell'\tau'\rangle$  the angular part given by:

$$|JMj\ell\tau\rangle = \sum_{mm_\ell} \langle jm\ell m_\ell | JM \rangle |j\tau m\rangle |m_\ell\rangle. \quad (11)$$

Introducing Eq. (10) in Eq. (8), we have to solve second-order coupled differential equations for the radial part of the wavefunctions:

$$\left[ \frac{d^2}{dr^2} - \frac{\ell'(\ell'+1)}{r^2} + \kappa_{j'\tau'}^2 \right] u_{j'\ell'\tau'}^{Jj\ell\tau}(r) = \frac{2\mu}{\hbar^2} \times \sum_{j''\ell''\tau''} \langle Jj'\tau'\ell' | V | JMj''\tau''\ell'' \rangle u_{j''\ell''\tau''}^{JMj\ell\tau}(r), \quad (12)$$

where  $\kappa_{j'\tau'}^2 = \frac{2\mu}{\hbar^2}(E_{\text{tot}} - E_{j'\tau'})$ . With the determination of these radial functions and knowing the asymptotic form of these functions, we can define the scattering matrix  $S^J$  by:

$$u_{j'\ell'\tau'}^{Jj\ell\tau}(r) \sim \delta_{jj'} \delta_{\tau\tau'} \delta_{\ell\ell'} \exp\left[-i\left(k_{j\tau}r - \frac{\ell\pi}{2}\right)\right] - \left(\frac{k_{j\tau}}{k_{j'\tau'}}\right)^{\frac{1}{2}} S_{j\tau\ell \rightarrow j'\tau'\ell'}^J \exp\left[i\left(k_{j\tau}r - \frac{\ell\pi}{2}\right)\right]. \quad (13)$$

Then the integral cross sections for the transition  $j\tau \rightarrow j'\tau'$  are given by:

$$\sigma_{j\tau \rightarrow j'\tau'} = \frac{\pi}{(2j+1)k_{j\tau}^2} \times \sum_{J=0}^{\infty} (2J+1) \sum_{\ell=|J-j|}^{J+j} \sum_{\ell'=|J-j'|}^{J+j'} |T_{j\tau\ell \rightarrow j'\tau'\ell'}^J|^2 \quad (14)$$

with  $T_{j\tau\ell \rightarrow j'\tau'\ell'}^J = \delta_{jj'} \delta_{\tau\tau'} \delta_{\ell\ell'} - S_{j\tau\ell \rightarrow j'\tau'\ell'}^J$ . The detailed balance is verified:

$$\sigma_{j'\tau' \rightarrow j\tau} = \frac{(2j+1)k_{j\tau}^2}{(2j'+1)k_{j'\tau'}^2} \sigma_{j\tau \rightarrow j'\tau'}. \quad (15)$$

This approach, known as the ‘‘close-coupling’’ method can be considered as exact, if one includes all the possible channels (open and closed). In practice one has to limit the number of channels, and it is important to check the convergence of such calculations and include a sufficient number of levels in the expansion. Other collision treatments are implemented in MOLSCAT, such as the coupled-states approximation introduced by McGuire & Kouri (1974). In this approximation,

**Table 4.** Values of the cross sections (in  $10^{-16}$  cm<sup>2</sup>) for some transitions of NH<sub>2</sub>D at a total energy of 100 cm<sup>-1</sup> with an increasing value of the number of rotational states included in the basis. For example B36 indicates a basis of 36 states.

Transition	B36	B49	B64	B81	B100
0 <sub>00</sub> → 1 <sub>01</sub>	0.6599	0.6565	0.6587	0.6584	0.6583
0 <sub>00</sub> → 1 <sub>10</sub>	0.9464	0.9375	0.9358	0.9363	0.9361
0 <sub>00</sub> → 2 <sub>02</sub>	1.0361	1.0366	1.0394	1.0396	1.0397
1 <sub>01</sub> → 0 <sub>00</sub>	0.2474	0.2462	0.2470	0.2469	0.2469
1 <sub>01</sub> → 1 <sub>11</sub>	0.4594	0.4619	0.4608	0.4615	0.4614
1 <sub>01</sub> → 1 <sub>10</sub>	0.4310	0.4365	0.4392	0.4394	0.4395
1 <sub>01</sub> → 2 <sub>02</sub>	3.6718	3.6777	3.6859	3.6889	3.6891
1 <sub>11</sub> → 1 <sub>01</sub>	0.4770	0.4795	0.4783	0.4791	0.4790
1 <sub>11</sub> → 1 <sub>10</sub>	0.2954	0.2906	0.2902	0.2899	0.2899
1 <sub>11</sub> → 2 <sub>02</sub>	0.4333	0.4314	0.4401	0.4405	0.4406

scattering equations are written in the BF frame, which is rotating. Then the projection of the orbital angular momentum is restricted to the value  $m_\ell = 0$ . This method gives satisfactory results as shown in Machin & Roueff (2005) for the NH<sub>3</sub>-He system and is much less expensive in CPU time. As the reduced mass of NH<sub>2</sub>D is larger than the reduced mass of NH<sub>3</sub>, more energy levels than in the NH<sub>3</sub>-He case have to be included for a given total collision energy. We used the coupled states approximation for data production after checking the validity of the approximation at some specific energies. The resulting uncertainty should not exceed a few percent on the computed collision rates.

#### 4. Calculations of the cross sections

We carefully checked the convergence of the S matrix for different collision parameters defined in MOLSCAT. The size of the basis set in the PES expansion, i.e., the number of  $v_{\lambda\mu}$  included in the calculations has been chosen to be 45 and includes terms up to  $\lambda = 8$  for energies up to 100 cm<sup>-1</sup>. At higher energies, 66 expansion coefficients have been introduced and include terms up to  $\lambda = 10$ . To illustrate this point we display some convergence tests for a total collision energy of 100 cm<sup>-1</sup> in Tables 4 and 5. On the other hand, 100 (144) rotational states have been included in the basis function for an energy of 100 (400) cm<sup>-1</sup> corresponding to a maximum energy of 830 (1224) cm<sup>-1</sup>.

We display the chosen input parameters used in MOLSCAT in Table 6. JTOTU = -1 means that MOLSCAT is checking itself for the convergence regarding the maximum  $J$  taken into account. Calculations have been performed for a total energy range between 11.1 cm<sup>-1</sup> and 400 cm<sup>-1</sup>. The energy step has been varied with increasing collision energy. It is 0.1 cm<sup>-1</sup> for a total energy range between 11.1 cm<sup>-1</sup> and 100 cm<sup>-1</sup>, 1 cm<sup>-1</sup> between 100 cm<sup>-1</sup> and 340 cm<sup>-1</sup>, and 5 cm<sup>-1</sup> between 340 cm<sup>-1</sup> and 400 cm<sup>-1</sup>.

Figure 3 illustrates the dependence of the 1<sub>11</sub> → 1<sub>01</sub> cross section as a function of the relative kinetic energy between NH<sub>2</sub>D and He. This transition at 85 GHz was first detected by Turner et al. (1978). A resonance structure is found at low energies. The peaks are due to the opening of new collision channels and correspond to so-called Feshbach resonances. Figure 4 displays a zoom of Fig. 3 in the energy range between 0 and 120 wavenumbers where the resonances appear. A small energy step is required in the calculations to fully account for the energy

**Table 5.** Values of the cross sections (in  $10^{-16}$  cm<sup>2</sup>) for some transitions of NH<sub>2</sub>D at a total energy of 100 cm<sup>-1</sup> with an increasing value of the number of radial coefficients  $v_{\lambda\mu}$  included in the expansion of the PES. For example L45 means that 45  $v_{\lambda\mu}$  were taken into account in the expansion.

Transition	L28	L45	L55
0 <sub>00</sub> → 1 <sub>01</sub>	0.6545	0.6583	0.6580
0 <sub>00</sub> → 1 <sub>10</sub>	0.9298	0.9361	0.9365
0 <sub>00</sub> → 2 <sub>02</sub>	1.0392	1.0397	1.0396
1 <sub>01</sub> → 0 <sub>00</sub>	0.2454	0.2469	0.2467
1 <sub>01</sub> → 1 <sub>11</sub>	0.4581	0.4614	0.4616
1 <sub>01</sub> → 1 <sub>10</sub>	0.4390	0.4395	0.4395
1 <sub>01</sub> → 2 <sub>02</sub>	3.6837	3.6892	3.6928
1 <sub>11</sub> → 1 <sub>01</sub>	0.4756	0.4790	0.4792
1 <sub>11</sub> → 1 <sub>10</sub>	0.2883	0.2899	0.2897
1 <sub>11</sub> → 2 <sub>02</sub>	0.4403	0.4406	0.4405

**Table 6.** Values of input parameters of MOLSCAT using in our calculations.

Parameter	Value
RMIN	3.0
INTFLG	6
STEPS	10.0
JTOTU	-1
NPTS	14, 14

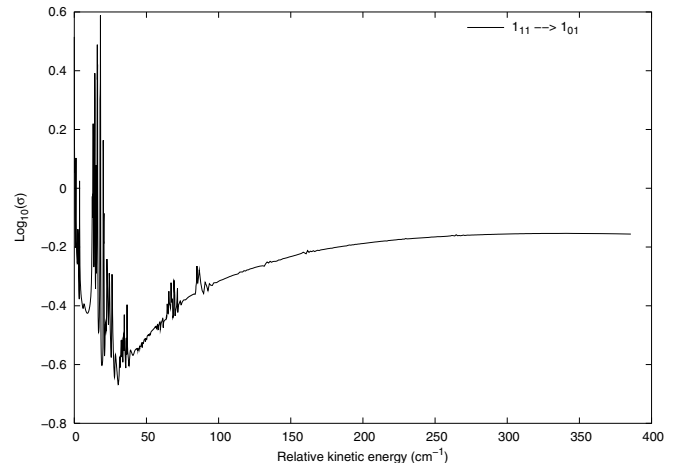


**Fig. 3.** Decimal logarithm of the cross section  $\sigma$  (in  $10^{-16}$  cm<sup>2</sup>) as a function of the relative kinetic energy for the transition 1<sub>11</sub> → 1<sub>01</sub> of NH<sub>2</sub>D.

dependence of the cross sections that may affect the results for the rate coefficients at very low temperatures.

#### 5. Rate coefficients for NH<sub>2</sub>D-He

The collisional (de)excitation rate coefficients in function of the temperature  $T$  are obtained via a Maxwellian average of the

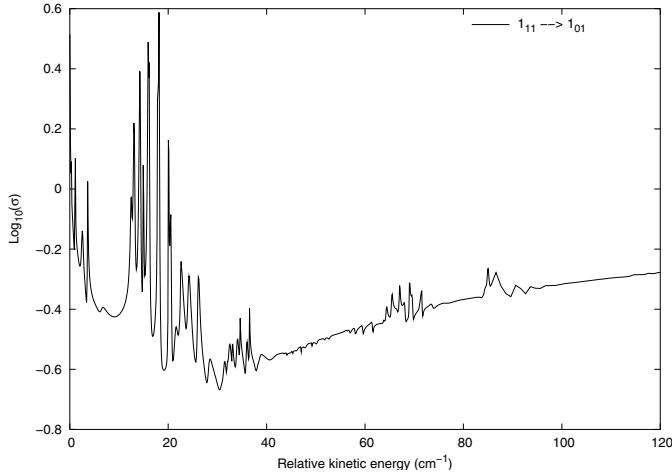


**Fig. 4.** Resonance structure in the cross section  $\sigma$  of the  $1_{11} \rightarrow 1_{01}$  transition. Decimal logarithm of  $\sigma$  (in  $10^{-16} \text{ cm}^2$ ) in function of the relative kinetic energy of NH<sub>2</sub>D and He.

cross sections times relative velocity. The integration formula is recalled below:

$$K_{j\tau \rightarrow j'\tau'}(T) = \left( \frac{8k_B T}{\pi\mu} \right)^{\frac{1}{2}} \left( \frac{1}{k_B T} \right)^2 \times \int_0^{\infty} \sigma_{j\tau \rightarrow j'\tau'}(E_{\text{tot}}) E \exp\left(-\frac{E}{k_B T}\right) dE, \quad (16)$$

where  $E$  is the relative kinetic energy,  $k_B$  is the Boltzmann constant, and  $\mu$  is the reduced mass of the NH<sub>2</sub>D-He system. As the integration should be performed until an infinite value of the relative kinetic energy, actual calculations introduce a maximum value that should be significantly larger than the mean thermal energy given approximately by  $k_B T$ , where the decreasing exponential brings a negligible contribution. As cross sections have only been computed until  $400 \text{ cm}^{-1}$ , we have calculated the rate coefficients for temperatures between 5 K and 100 K that are relevant for the interstellar medium. We show the effect of the energy cut-off on the computed rate coefficients in Fig. 5. In this figure, we see that the rate coefficients of the  $1_{11} \rightarrow 1_{01}$  transition are identical for temperatures between 5 and 20 K, whatever value is used for the energy cut-off. However, the situation is somewhat different for higher temperatures where the values obtained for the rate coefficients are quite different for a low value of the cut-off. We estimate that the convergence is attained at 100 K when we integrate Eq. (16) until  $E = 400 \text{ cm}^{-1}$ , as the differences between the rate coefficients become quite close for maximum energy values of 300, 350, and  $400 \text{ cm}^{-1}$ . We estimate that the resulting error is of the order of 3%.

We have also checked the detailed balance via independent integrations of the excitation and de-excitation cross-sections to validate our results. The detailed balance conditions on the rate coefficients are then verified with an error that does not exceed 1% at the lower temperatures and 0.1% at the higher temperatures. We display the values of the rate coefficients corresponding to transitions of NH<sub>2</sub>D induced by He collisions, involving the lowest energy levels for temperatures between 5 and 100 K in Table 7. The temperature variation is smooth, as one can see from the values displayed in Table 7, and collisional de-excitation rate coefficients slightly increase with temperature.

Molecular hydrogen is the main constituent of interstellar molecular clouds and the interpretation of astrophysical spectra requires knowledge of collision rates of molecules with

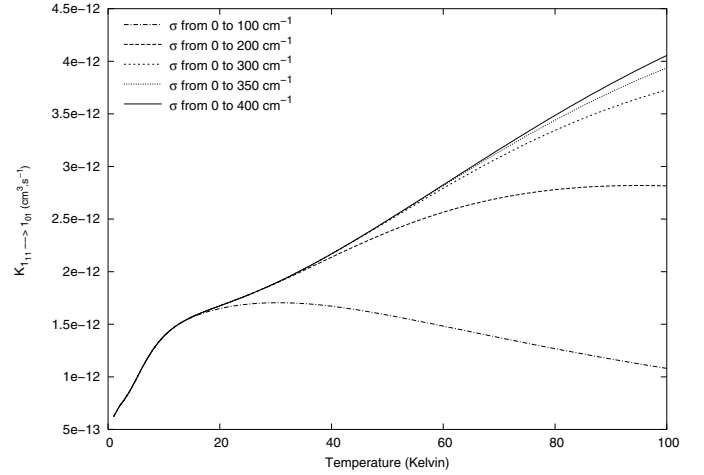


**Fig. 5.** Rate coefficients  $K_{1_{11} \rightarrow 1_{01}}$  ( $\text{cm}^3 \text{ s}^{-1}$ ) of the transition  $1_{11} \rightarrow 1_{01}$  in function of the temperature obtained for different values of the maximum total energy in the integration performed in Eq. (16):  $100 \text{ cm}^{-1}$ ,  $200 \text{ cm}^{-1}$ ,  $300 \text{ cm}^{-1}$ ,  $350 \text{ cm}^{-1}$ , and  $400 \text{ cm}^{-1}$ .

molecular hydrogen. Helium is often considered as a prototype of molecular hydrogen in its para form,  $j = 0$ , which is probably the most abundant populated level in cold dark interstellar clouds. Then, rate coefficients for NH<sub>2</sub>D-para-H<sub>2</sub> can be tentatively deduced from those involving He, if one assumes that the collision probabilities are identical. The values of the rate coefficients of NH<sub>2</sub>D-H<sub>2</sub> may then be estimated as the product of the rate coefficients for NH<sub>2</sub>D-He by the square root of the ratio of the reduced masses (here 1.3441).

Astrophysicists define a critical density corresponding to a specific transition as the ratio between the Einstein coefficients  $A_{if}$  and the rate coefficients  $K_{if}$  for a specific collider. This value sets the limit of the perturber density above which the transitions are thermalized. Table 8 displays the estimated values of the critical densities of H<sub>2</sub> thus derived for some specific transitions. We see that the critical density corresponding to the 85 GHz transition ( $1_{10} \rightarrow 1_{11}$ ) is of the order of  $2 \times 10^4 \text{ cm}^{-3}$ , whereas those corresponding to higher frequency transitions involving the ground rotational level attain values larger than  $10^6 \text{ cm}^{-3}$ .

## 6. Conclusions

Rotational excitation cross sections of NH<sub>2</sub>D induced by He collisions are presented for the first time. Calculations have been performed in the quantal CS approximation by including the couplings arising from the change of the reference frame from the NH<sub>3</sub>-He system. The total collision energy range is extending from  $11.1 \text{ cm}^{-1}$  to  $400 \text{ cm}^{-1}$ . Collision rate coefficients have been derived for temperatures relevant to interstellar conditions, from 5 K to 100 K. Deuteration fractionation processes may take place in low temperature conditions where deuterated isotopologs are detected. The values of the rate coefficients are available on request to the authors and will be part of the Basecol database<sup>1</sup>. Similar computations are performed for ND<sub>2</sub>H perturbed by He. These values may also be used as a first guess to derive NH<sub>2</sub>D rotational excitation due to para-H<sub>2</sub> in astrophysical applications by using the weighting factor 1.3441 deduced from reduced mass effects. Calculations involving the appropriate PES are under way.

<sup>1</sup> Basecol, <http://amdpo.obspm.fr/basecol>

**Table 7.** Einstein coefficients and rate coefficients for NH<sub>2</sub>D-He for different temperatures. Only de-excitation transitions are considered. Numbers in parentheses correspond to the power of ten. Einstein coefficients are taken from the CDMS database (Müller et al. 2001) and are given for the *ortho* and *para* transitions.

Transition	Einstein coefficients $A_{if}$ (s <sup>-1</sup> )		Rate coefficients $K_{if}$ (cm <sup>3</sup> s <sup>-1</sup> )					
	<i>ortho</i>	<i>para</i>	5 K	10 K	25 K	50 K	75 K	100 K
1 <sub>01</sub> → 0 <sub>00</sub>	7.82(-6)	7.29(-6)	7.56(-13)	7.75(-13)	1.04(-12)	1.41(-12)	1.70(-12)	1.90(-12)
1 <sub>11</sub> → 1 <sub>01</sub>	7.82(-6)	1.65(-5)	9.74(-13)	1.39(-12)	1.78(-12)	2.49(-12)	3.33(-12)	4.06(-12)
1 <sub>10</sub> → 0 <sub>00</sub>	8.55(-4)	9.95(-4)	9.56(-13)	9.83(-13)	1.29(-12)	1.94(-12)	2.58(-12)	3.09(-12)
1 <sub>10</sub> → 1 <sub>01</sub>	–	–	4.47(-12)	3.95(-12)	3.50(-12)	3.48(-12)	3.60(-12)	3.72(-12)
1 <sub>10</sub> → 1 <sub>11</sub>	4.36(-8)	4.05(-8)	1.42(-12)	1.41(-12)	1.48(-12)	1.82(-12)	2.16(-12)	2.43(-12)
2 <sub>02</sub> → 0 <sub>00</sub>	–	–	2.42(-12)	2.34(-12)	2.17(-12)	2.23(-12)	2.39(-12)	2.52(-12)
2 <sub>02</sub> → 1 <sub>01</sub>	–	–	1.51(-11)	1.51(-11)	1.61(-11)	1.92(-11)	1.92(-11)	2.36(-11)
2 <sub>02</sub> → 1 <sub>11</sub>	–	–	2.45(-12)	2.37(-12)	2.28(-12)	2.34(-12)	2.46(-12)	2.56(-12)
2 <sub>02</sub> → 1 <sub>10</sub>	1.57(-4)	1.35(-4)	2.72(-13)	3.21(-13)	3.31(-13)	3.60(-13)	4.26(-13)	4.89(-13)
2 <sub>12</sub> → 1 <sub>01</sub>	–	–	1.22(-12)	1.11(-12)	9.63(-13)	9.67(-13)	1.03(-12)	1.10(-12)
2 <sub>12</sub> → 1 <sub>11</sub>	–	–	1.51(-11)	1.39(-11)	1.41(-11)	1.68(-11)	1.93(-11)	2.11(-11)
2 <sub>12</sub> → 1 <sub>10</sub>	–	–	4.68(-14)	7.87(-14)	1.48(-13)	2.40(-13)	3.81(-13)	5.26(-13)
2 <sub>12</sub> → 2 <sub>02</sub>	1.81(-6)	5.92(-6)	1.38(-12)	1.51(-12)	2.06(-12)	3.07(-12)	4.09(-12)	4.92(-12)
2 <sub>11</sub> → 0 <sub>00</sub>	–	–	1.02(-12)	1.01(-12)	1.06(-12)	1.25(-12)	1.46(-12)	1.63(-12)
2 <sub>11</sub> → 1 <sub>01</sub>	4.62(-3)	5.02(-3)	1.58(-12)	1.57(-12)	1.79(-12)	2.39(-12)	2.97(-12)	3.43(-12)
2 <sub>11</sub> → 1 <sub>11</sub>	–	–	3.50(-11)	3.57(-11)	3.64(-11)	3.83(-11)	3.95(-11)	3.98(-11)
2 <sub>11</sub> → 1 <sub>10</sub>	6.49(-5)	7.07(-5)	1.07(-12)	1.08(-12)	1.29(-12)	1.80(-12)	2.30(-12)	2.68(-12)
2 <sub>11</sub> → 2 <sub>02</sub>	–	–	3.01(-12)	2.82(-12)	2.31(-12)	2.23(-12)	2.38(-12)	2.56(-12)
2 <sub>11</sub> → 2 <sub>12</sub>	4.16(-7)	6.42(-7)	4.48(-12)	5.28(-12)	8.09(-12)	1.21(-11)	1.52(-11)	1.74(-11)
2 <sub>21</sub> → 1 <sub>01</sub>	–	–	2.59(-11)	2.65(-11)	2.78(-11)	3.01(-11)	3.18(-11)	3.27(-11)
2 <sub>21</sub> → 1 <sub>11</sub>	–	–	2.89(-12)	2.85(-12)	3.09(-12)	3.69(-12)	4.29(-12)	4.73(-12)
2 <sub>21</sub> → 1 <sub>10</sub>	–	–	8.32(-13)	8.46(-13)	8.48(-13)	9.09(-13)	9.85(-13)	1.05(-12)
2 <sub>21</sub> → 2 <sub>02</sub>	–	–	4.96(-12)	5.23(-12)	6.35(-12)	8.25(-12)	9.85(-12)	1.10(-11)
2 <sub>21</sub> → 2 <sub>12</sub>	–	–	3.57(-12)	3.54(-12)	3.60(-12)	4.14(-12)	4.89(-12)	5.55(-12)
2 <sub>21</sub> → 2 <sub>11</sub>	1.18(-4)	9.22(-5)	1.20(-12)	1.30(-12)	1.59(-12)	2.13(-12)	2.66(-12)	3.06(-12)
2 <sub>20</sub> → 0 <sub>00</sub>	–	–	9.52(-12)	9.51(-12)	1.01(-11)	1.17(-11)	1.30(-11)	1.38(-11)
2 <sub>20</sub> → 1 <sub>01</sub>	–	–	9.54(-13)	1.00(-12)	1.24(-12)	1.61(-12)	1.91(-12)	2.12(-12)
2 <sub>20</sub> → 1 <sub>11</sub>	–	–	1.06(-12)	1.09(-12)	1.19(-12)	1.35(-12)	1.50(-12)	1.60(-12)
2 <sub>20</sub> → 1 <sub>10</sub>	–	–	3.38(-12)	3.30(-12)	3.51(-12)	4.28(-12)	5.04(-12)	5.61(-12)
2 <sub>20</sub> → 2 <sub>02</sub>	–	–	2.18(-11)	2.13(-11)	1.97(-11)	1.90(-11)	1.89(-11)	1.87(-11)
2 <sub>20</sub> → 2 <sub>12</sub>	2.09(-4)	1.79(-4)	9.86(-13)	1.01(-12)	9.74(-13)	1.10(-12)	1.27(-12)	1.41(-12)
2 <sub>20</sub> → 2 <sub>11</sub>	–	–	2.68(-12)	2.67(-12)	2.66(-12)	2.93(-12)	3.33(-12)	3.68(-12)
2 <sub>20</sub> → 2 <sub>21</sub>	1.46(-9)	1.52(-9)	2.42(-12)	2.42(-12)	2.44(-12)	2.97(-12)	3.62(-12)	4.15(-12)

**Table 8.** Critical density for some *ortho* and *para* transitions of NH<sub>2</sub>D with H<sub>2</sub>. Collision rate coefficients for NH<sub>2</sub>D-H<sub>2</sub> are those for NH<sub>2</sub>D-He multiplied by the reduced masses ratio of 1.3441. Densities are in cm<sup>-3</sup>.

Transition	Critical density (cm <sup>-3</sup> )	
	<i>ortho</i>	<i>para</i>
1 <sub>01</sub> → 0 <sub>00</sub>	7.51 × 10 <sup>6</sup>	7.00 × 10 <sup>6</sup>
1 <sub>11</sub> → 1 <sub>01</sub>	4.19 × 10 <sup>6</sup>	8.85 × 10 <sup>6</sup>
1 <sub>10</sub> → 0 <sub>00</sub>	6.47 × 10 <sup>8</sup>	7.51 × 10 <sup>8</sup>
1 <sub>10</sub> → 1 <sub>11</sub>	2.30 × 10 <sup>4</sup>	2.14 × 10 <sup>4</sup>
2 <sub>02</sub> → 1 <sub>10</sub>	3.64 × 10 <sup>8</sup>	3.13 × 10 <sup>8</sup>
2 <sub>12</sub> → 2 <sub>02</sub>	8.93 × 10 <sup>5</sup>	2.92 × 10 <sup>6</sup>
2 <sub>11</sub> → 1 <sub>01</sub>	2.19 × 10 <sup>9</sup>	2.38 × 10 <sup>9</sup>
2 <sub>11</sub> → 1 <sub>10</sub>	4.47 × 10 <sup>7</sup>	4.87 × 10 <sup>7</sup>
2 <sub>11</sub> → 2 <sub>12</sub>	5.86 × 10 <sup>4</sup>	9.08 × 10 <sup>4</sup>
2 <sub>21</sub> → 2 <sub>11</sub>	6.76 × 10 <sup>7</sup>	5.27 × 10 <sup>7</sup>
2 <sub>20</sub> → 2 <sub>12</sub>	1.54 × 10 <sup>8</sup>	1.32 × 10 <sup>8</sup>
2 <sub>20</sub> → 2 <sub>21</sub>	4.48 × 10 <sup>2</sup>	4.67 × 10 <sup>2</sup>

**Acknowledgements.** We are grateful to Marie-Lise Dubernet of LERMA-Meudon and Pierre Valiron of the Laboratoire d'Astrophysique de Grenoble for useful discussions. This work is one of the tasks defined in the European FP6 network "The Molecular Universe".

## References

- Benedict, W. S., Gailar, N., & Plyler, E. K. 1957, *Can. J. Phys.*, 35, 1235  
 Cheung, A. C., Rank, D. M., Townes, C. H., Thornton, D. D., & Welch, W. J. 1968, *Phys. Rev. Lett.*, 21, 1701  
 Cohen, A. E., & Pickett, H. M. 1982, *J. Mol. Spectrosc.*, 93, 83  
 Coudert, L., & Roueff, E. 2006, *Astron. & Astrophys.*, 449, 855  
 Coudert, L., Valentin, A., & Henry, L. 1986, *J. Mol. Spectrosc.*, 120, 185  
 Garrison, B. J., Lester, W. A., & Miller, W. H. 1976, *J. Chem. Phys.*, 65, 2193  
 Garrison, B. J., & Lester, W. A. 1977, *J. Chem. Phys.*, 66, 531  
 Green, S. 1976, *J. Chem. Phys.*, 64, 3463  
 Hodges, M. P., & Wheatley, R. J. 2001, *J. Chem. Phys.*, 114, 8836  
 Larsson, B., Liseau, R., Bergman, P., et al. 2003, *A&A*, 402, L69  
 Liseau, R., Larsson, B., Brandeker, A., et al. 2003, *A&A*, 402, L73  
 Machin, L., & Roueff, E. 2005, *J. Phys. B: At. Mol. Opt. Phys.*, 38, 1519  
 McGuire, P., & Kouri, D. J. 1974, *J. Chem. Phys.*, 60, 2488  
 Hutson, J. M., & Green, S. 1995, MOLSCAT computer code, version 14, distributed by collaborative computational project No. 6 of the Science and Engineering Research Council, UK  
 Müller, H. S. P., Thorwirth, S., Roth, D. A., & Winnewisser, G. 2001, *A&A*, 370, L49  
 Palma, A., & Green, S. 1987, *ApJ*, 316, 83  
 Saito, S., Ozeki, H., Ohishi, M., & Yamamoto, S. 2000 *ApJ*, 535, 227  
 Shah, R. Y., & Wootten, A. 2001, *ApJ*, 554, 933  
 Tiné, S., Roueff, E., Falgarone, E., Gerin, M., & Pineau des Forêts, G. 2000, *A&A*, 356, 1039  
 Townes, C. H., & Schawlow, A. L. 1975, *Microwave Spectroscopy* (New York: Dover Publications)  
 Turner, B. E., Zuckerman, B., Morris, M., & Palmer, P. 1978, *ApJ*, 219, L43